# Resonant drift of two-armed spirals by a periodic advective field and periodic modulation of excitability

Ling-Yun Deng, Hong Zhang,[*] and You-Quan Li

*Zhejiang Institute of Modern Physics and Department of Physics, Zhejiang University, Hangzhou 310027, China*
(Received 18 May 2009; revised manuscript received 15 July 2009; published 8 January 2010)

The drift behavior of two-armed spirals induced by periodic advective field and periodic modulation of excitability is investigated. It is shown that the two-armed spirals controlled by periodic advective field and periodic modulation of excitability drift in completely different ways. For periodic advective field, the two tips of the two-armed spiral drift in the same direction and the two-armed spiral is stable. While for periodic modulation of excitability, the two tips drift in the opposite direction and the two-armed spiral splits into two single-armed spirals. Analytical results based on a kinematic theory of rotating spirals in weakly excitable media are consistent with the numerical results.

## I. INTRODUCTION

Spiral waves are known to exist in spatially distributed chemical and biological systems belonging to the class of excitable media [1–5]. A spiral wave is a self-sustained wave that rotates freely or around some obstacle. In cardiology, it is thought that spiral waves are responsible for many dangerous cardiac arrhythmias and are precursors of ventricular fibrillation and subsequent sudden death [6–10]. Thus, it is important to know how to control spiral waves so that we can prevent or suppress them.

Multiarmed spiral is an ensemble of same-chirality spiral waves whose tips are separated by less than a core diameter [11–19]. They have been observed in Belousov-Zhabotinsky (BZ) reaction [11], Dictyostelium discoideum [14], the whole rabbit heart [15], two-dimensional cultured heart tissue [16], and a variety of numerical reaction-diffusion models of excitable media [18,19].

In the study of the control of spiral waves, an active field of recent investigation concerns the resonant drift of the spiral core induced by periodic forcing [20] and advective field [21]. For spiral waves, resonant drift corresponds to a net drift of the rotation centers along a straight line. Agladze *et al.* [22] reported the first experimental observation of a drift of spiral waves during periodic modulation of the excitability of an excitable medium with a frequency close to the nature rotation frequency of the spiral waves. In the presence of a dc electric field, Steinbock *et al.* [23] showed that the center of spiral waves in the BZ reaction drifts with a velocity whose two components are parallel and perpendicular to the applied field. In Ref. [24], Muñuzuri *et al.* observed that the spiral in the BZ reaction undergoes a directional drift when the frequency of an ac electric field is twice that of the spiral frequency. However, all these works considered only one-armed spirals while the drift of multiarmed spirals induced by external actions has not been investigated yet. In this paper, we will investigate the drift of two-armed spirals under the influence of periodic advective field and periodic modulation of excitability.

---

*Author to whom correspondence should be addressed. hongzhang@zju.edu.cn; hzhang@zimp.zju.edu.cn

## II. NUMERICAL RESULTS

All observations were made in numerical simulations in a modified FitzHugh-Nagumo model [25]. This model consists of an activator variable $u$ and an inhibitor variable $v$, which evolve according to

$$\frac{\partial u}{\partial t} = \frac{f(u,v)}{\epsilon} + \nabla^2 u, \tag{1}$$

$$\frac{\partial v}{\partial t} = g(u,v), \tag{2}$$

where $f(u,v) = u(1-u)[u-(v+b)/a]$ and $g(u,v) = u-v$ characterizing the dynamics of the medium; the constant $\epsilon$ denotes the ratio of characteristic time scales of the activator and inhibitor variables; the parameters $a$ and $b$ represent the slope of the $u$ nullcline and the excitation threshold.

### A. Two-armed spirals

Numerical simulations are carried out on $1000 \times 1000$ grid points employing the explicit Euler method. The space and time steps are $\Delta x = \Delta y = 0.1826$ and $\Delta t = 0.005$, respectively. No-flux conditions are imposed at the boundaries. A two-armed spiral is initiated by superimposing snapshots of a single-armed spiral in equally spaced phases [19]. In Fig. 1,
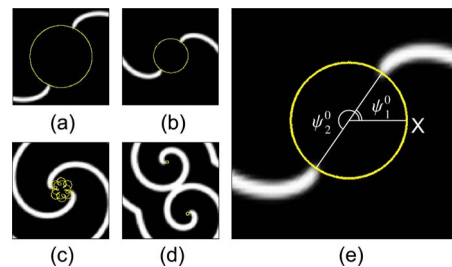


FIG. 1. (Color online) Tip trajectories of two-armed spiral waves. (a) $b=0.245$, (b) $b=0.24$, (c) $b=0.22$, (d) $b=0.2$, (e) the initial phases of two spiral tips $\psi_1^0$ and $\psi_2^0$ of a counterclockwise rotating two-armed spiral. The tip of the spiral wave is defined as the intersection of contour lines $u=0.3$ and $v=0.3$.

the dynamics of two-armed spiral waves is investigated by varying $b$ and fixing $\epsilon=0.02$ and $a=1.1$. One can see that for $b<0.21$, the initial two-armed spiral is not stable and will decay into two single-armed spirals, for more details, see Fig. 1(a) of Ref. [26]. It was shown in [26] that the average period, as an important quantity of multiarmed spiral, must be larger than a threshold for stable multiarmed spiral. The average period of the two-armed spiral decreases as we diminish $b$ [26]. Once the average period is lower than a threshold (where $b=0.21$), the two-armed spiral will not be stable any more, and it will decay into two single-armed spirals [see Fig. 1(d)]. In Ref. [19], the authors explore the phase diagram of multiarmed spiral in the plane of parameters $a$-$b$; the multiarmed spiral state exists only in a stripe-like region. In this paper, we choose $\epsilon=0.02$, $a=1.1$, and $b=0.24$ for all simulations. For these parameters, the excitability of systems (1) and (2) is weak and the system has a rigidly rotating two-armed spiral solution [see Fig. 1(b)]. The initial phases of two spiral tips $\psi_j^0$ ($j=1,2$, $\psi_2^0-\psi_1^0\simeq\pi$) of a rigidly rotating two-armed spiral are defined in Fig. 1(e).

### B. Periodic advective field

Now we investigate the response of a two-armed spiral under the influence of a periodic advective field. In the presence of a periodic advective field $E=E_f\cos(\omega_e t+\varphi)$ which couples to the activator $u$, the activator reaction-diffusion equation becomes

$$\frac{\partial u}{\partial t}=\frac{f(u,v)}{\epsilon}+\nabla^2 u+E\frac{\partial u}{\partial x}. \qquad (3)$$

In Refs. [24,27,28], it was shown that a rigidly rotating single-armed spiral drifts when the frequency of the periodic advective field is twice that of the single-armed spiral, i.e., $\omega_e=2\omega_0$ ($\omega_0$ is the angular frequency of the spiral and it will change under external actions). So, we will consider the influence of a periodic advective field with $\omega_e=2\omega_0$ on the dynamics of a two-armed spiral firstly. Our numerical simulations show that the two tips of the two-armed spiral drift in the same direction and the two-armed spiral is still stable. The corresponding trajectories of the two tips are shown in Fig. 2(a). $\Theta_1$ and $\Theta_2$ are the drift directions of the two tips, respectively. There is a small difference between the $\Theta_1$ and $\Theta_2$. This is due to the fact that the two tips are not separated in equal phase precisely because of the discreteness of time and space in numerical simulations.

The two-armed spiral will drift in different directions when we change the initial phases of spiral tips $\psi_j^0$, as shown in Figs. 2(b)–2(d). One can see that the change of drift direction $\Theta_j$ ($j=1,2$) is twice as much as that of $\psi_j^0$, i.e., $|\Delta\Theta_j|=2|\Delta\psi_j^0|$, see Fig. 2(b) for details. Thus $|\Delta\Theta_j|=2\pi$ if $|\Delta\psi_j^0|=\pi$; this means that the drift direction $\Theta_j$ keeps invariant when the change of $\psi_j^0$ is $\pi$ (or $-\pi$) [see Figs. 2(c) and 2(d)].

In above discussions, only resonant drift ($\omega_e=2\omega_0$) of two-armed spirals under periodic advective field are investigated. It is also interesting to study what happens when two-armed spirals are induced by a periodic advective field with $\omega_e\neq2\omega_0$. Our numerical results show that the two-armed
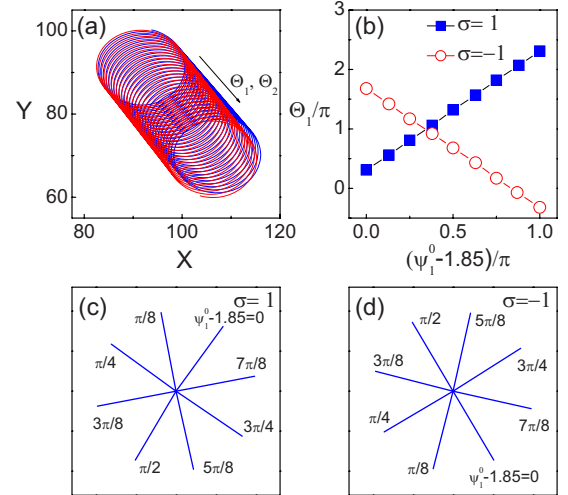


FIG. 2. (Color online) (a) The trajectories of the two tips of a clockwise rotating two-armed spiral ($\sigma=-1$) controlled by a periodic advective field with $\omega_e=2\omega_0$, $E_f=0.01$. $\Theta_1$ and $\Theta_2$ are the drift directions of the two tips, respectively. [(b)–(d)] Variation of the drift direction $\Theta_1$ with $\psi_1^0$. $\sigma=\pm1$ represent the chirality of the spiral, $\sigma=1$ for counterclockwise rotating spiral, while $\sigma=-1$ for the clockwise one.

spiral do not drift under periodic advective field with $\omega_e\neq2\omega_0$. For examples, we give the dynamics of a two-armed spiral controlled by periodic advective field with $\omega_e=\omega_0$, $1.5\omega_0$, $2.5\omega_0$, and $3\omega_0$ in Fig. 3. The tips of the two-armed spiral do not drift but rotate around the center.

### C. Periodic modulation of excitability

The excitability of the medium is modulated periodically by setting the parameter $b=b_0+b_f\cos(\omega_b t+\varphi)$. The activator reaction-diffusion equation becomes
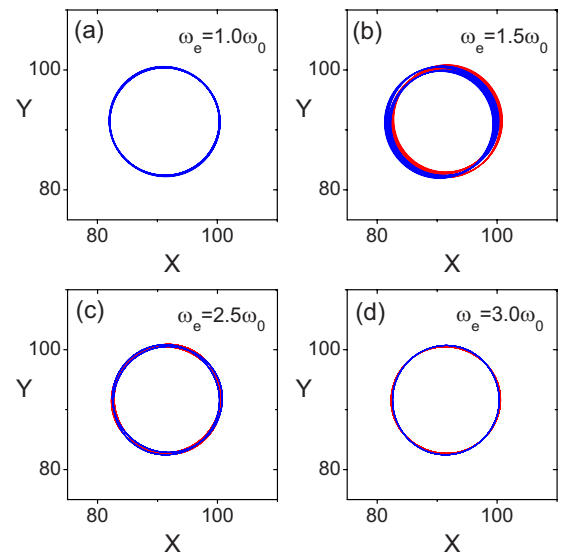


FIG. 3. (Color online) The trajectories of the two tips of a clockwise rotating two-armed spiral ($\sigma=-1$) controlled by a periodic advective field ($E_f=0.01$) with (a) $\omega_e=\omega_0$, (b) $\omega_e=1.5\omega_0$, (c) $\omega_e=2.5\omega_0$, (d) $\omega_e=3\omega_0$. The total time of the simulations is 500.
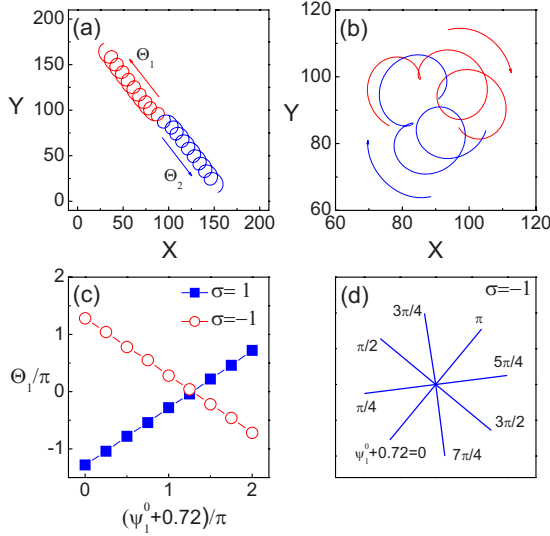
FIG. 4. (Color online) (a) The trajectories of the two tips of a clockwise rotating two-armed spiral when the excitability of the medium is modulated periodically with $\omega_b = \omega_0$, $b_f = 0.0035$. $\Theta_1$ and $\Theta_2$ are the drift directions of the two tips, respectively. The two tips drift in the opposite direction and the two-armed spiral splits into two single-armed spirals. (b) The trajectories of the two tips of a two-armed spiral with resonant modulation with $b_f = 0.0027$. Two-armed spiral cannot be split into two single-armed spirals. [(c) and (d)] Variation of $\Theta_1$ with $\psi_1^0$. The parameter are $b_f = 0.003$, $\omega_b = \omega_0$.

$$\frac{\partial u}{\partial t} = \left. \frac{f(u,v)}{\epsilon} \right|_{b_0} + \nabla^2 u - \frac{1}{\epsilon} \frac{u(1-u)}{a} b_f \cos(\omega_b t + \varphi). \quad (4)$$

In Refs. [22,29,30], it was shown that a rigidly rotating single-armed spiral drifts when the frequency of the modulation is equal to that of the single-armed spiral. Here, we will firstly investigate the dynamics of a two-armed spiral induced by periodic modulation of excitability with $\omega_b = \omega_0$. Figure 4(a) shows the tips trajectories of a two-armed spiral when the medium is resonantly modulated. The two tips drift in the opposite direction ($\Theta_2 - \Theta_1 \simeq \pi$) and the two-armed spiral split into two single-armed spirals. In Figs. 4(c) and 4(d), we plot the relation between the drift direction and the initial phase of one of the spiral tips. Different from the case of periodic advective field, the change of drift direction $\Theta_j$ is equal to that of $\psi_j^0$, i.e., $|\Delta\Theta_j| = |\Delta\psi_j^0|$. This means that the drift direction $\Theta_j$ keeps invariant when the change of $\psi_j^0$ is $2\pi$ (or $-2\pi$), see Fig. 4(d) for details.

However, when the amplitude of modulation is weak ($b_f \lesssim 0.0027$), the two-armed spiral is not split into two single-armed spirals by periodic modulation of excitability with $\omega_b = \omega_0$. In this case the two tips meander around each other, see Fig. 4(b). Our numerical results show that the two-armed spiral can be split into two single-armed spirals when $b_f \gtrsim 0.0028$. Therefore we suppose that one may estimate the strength of the interaction between the arms of a multiarmed spiral by measuring the smallest amplitude of modulation $b_f$ that can split a multiarmed spiral.

We also study the dynamics of the two-armed spiral when $\omega_b \neq \omega_0$. In Fig. 5, for examples, we give the dynamics of a
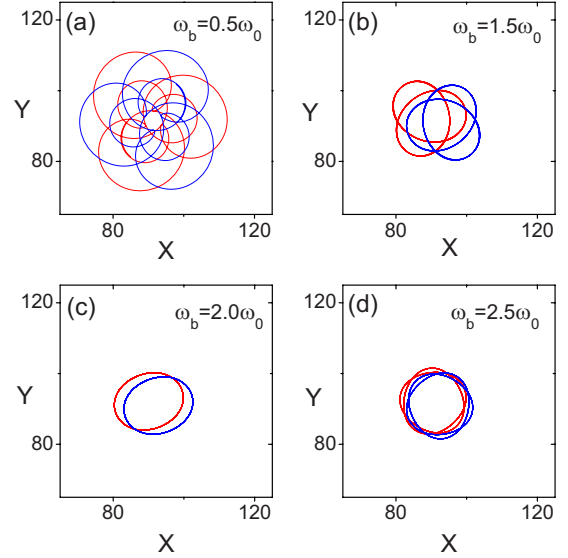


FIG. 5. (Color online) The trajectories of the two tips of a clockwise rotating two-armed spiral ($\sigma = -1$) when the excitability of the medium is modulated periodically ($b_f = 0.003$) with (a) $\omega_b = 0.5\omega_0$, (b) $\omega_b = 1.5\omega_0$, (c) $\omega_b = 2\omega_0$, (d) $\omega_b = 2.5\omega_0$. The total time of the simulations is 500.

two-armed spiral under periodic modulation of excitability with $\omega_b = 0.5\omega_0$, $1.5\omega_0$, $2\omega_0$, and $2.5\omega_0$. The tips of the two-armed spiral do not drift but meander.

For $\omega_b = 0.5\omega_0$, second-order resonant drift of single-armed spiral has been observed [13,31] in a surface chemical reaction of CO oxidation and has been derived [29] in the framework of a kinematic theory. Here, we do not observe the second-order resonant drift of two-armed spirals [Fig. 5(a)] perhaps due to the interaction between the arms.

## III. ANALYTIC METHODS

A kinematical model of spiral dynamics, aimed at the weakly excitable large core limit, was proposed on a phenomenological basis [29]. It has been helpful to rationalize experimental facts. In Ref. [27], an asymptotic derivation of a kinematic theory of spiral wave motion in the weakly excitable and free-boundary limit was presented. In this section, we will explain our numerical results using the kinematic theory developed in [27]. The interaction between spiral arms is caused by the unrecovered disturbance left by former wave. Since the period of spiral waves is quite long in the weak excitability limit, the interaction between spiral arms of a two-armed spiral will be neglected in the following analysis, for simplicity.

Consider a rigidly rotating two-armed spiral, the motion of the $j$th tip obeys

$$z_j(t) = R_0 e^{i\sigma(\omega_0 t + \psi_j^0)}, \quad j = 1, 2, \quad (5)$$

where $z_j(t) = x_j(t) + iy_j(t)$ is the position of the $j$th spiral tip. Equation (5) describes a two-armed spiral whose tips rotates steadily at a frequency $\omega_0$ around a circular core of radius $R_0$. Here $\sigma = \pm 1$ represent the chirality of the spiral, $\sigma = 1$ for counterclockwise rotating spiral, while $\sigma = -1$ for the clock-

wise one. $\psi_j^0$ denotes the initial phase of the $j$th tip. For a rigidly rotating two-armed spiral separated in equal phase, we have $\psi_2^0 - \psi_1^0 \simeq \pi$ [see Fig. 1(e)].

Kinematically, the motion of the $j$th tip of a two-armed spiral which is displaced from its steady-state position can be written as

$$z_j = [R_0 + r_j(t)]e^{i\sigma[\omega_0 t + \psi_j(t)]}, \tag{6}$$

where $\sigma[\omega_0 t + \psi_j(t)]$ is the phase angle of the $j$th tip, $r_j(t)$ a slight displacement from its rigid rotating radius $R_0$, and $\psi_j(0) = \psi_j^0$. According to [27], the equation for the radial motion of the $j$th tip satisfies

$$\ddot{r}_j + \omega_0^2 r_j = \omega_0^2 \delta R_j, \tag{7}$$

where $R_j$ is the instantaneous radius of curvature of the $j$th tip trajectory.

When the medium is submitted to a periodic advective field $E = E_f \cos(\omega_e t + \varphi)$, the influence of the advective field on tangential velocity of spiral tip takes the form of $\delta c_t = \gamma_\| E_\| + \gamma_\perp E_\perp$. Then we have

$$\delta R_j = \left. \frac{\partial R_j}{\partial c_t} \right|_{c_t^0} (\gamma_\| E_\| + \gamma_\perp E_\perp). \tag{8}$$

Here $c_t^0$ is the tangential velocity of the spiral tip without external fields. Coefficients $\gamma_\|$ and $\gamma_\perp$ are determined by the properties of the medium, and can be expressed as $\gamma_\| = \gamma \cos(\Phi)$, $\gamma_\perp = \gamma \sin(\Phi)$ with $\Phi = \arctan(\gamma_\perp / \gamma_\|)$ a constant. $E_\| = -E \sin(\omega_0 t + \psi_j^0)$ and $E_\perp = E \cos(\omega_0 t + \psi_j^0)$ are the advective field component, respectively, parallel and orthogonal to the tangential tip velocity.

The relation between $R_j$ and $c_t$ has been given in [27]. Therefore we have $\partial R_j / \partial c_t |_{c_t^0} = 3R_0/[2(c_0 - c_t^0)]$, where $c_0$ is the propagating velocity of plane wave. The solution of Eq. (7) for a periodic advective field $E = E_f \cos(\omega_e t + \varphi)$ with $\omega_e = 2\omega_0$ is given by

$$\frac{r_j(t)}{R_0} = -\frac{3}{8} \frac{\gamma E_f}{(c_0 - c_t^0)} \omega_0 t \cos(\omega_0 t + \varphi + \Phi - \psi_j^0)$$

$$+ \frac{3}{32} \frac{\gamma E_f}{(c_0 - c_t^0)} \sin(3\omega_0 t + \varphi - \Phi + \psi_j^0). \tag{9}$$

The displacement $r_j(t)$ describes the $j$th tip drifting away from the origin at a constant velocity combined with a circular motion. Therefore the drift of the rotation center of the $j$th tip can be written as

$$z_j^0(t) = \frac{3}{8} \frac{\gamma E_f R_0}{(c_0 - c_t^0)} \omega_0 t \exp[i\sigma(\pi - \varphi - \Phi + 2\psi_j^0)]. \tag{10}$$

One can see that the drift direction $\Theta_j$ is equal to $\sigma(\pi - \varphi - \Phi + 2\psi_j^0)$, and thus we have

$$|\Delta \Theta_j| = 2|\Delta \psi_j^0|. \tag{11}$$

This can explain our numerical results observed in Figs. 2(b)–2(d). In Figs. 6(a) and 6(b), we also give the relation between the drift direction and the initial phase of a single-armed spiral. The numerical results agrees well with the analytic results. For a rigidly rotating two-armed spiral with tips
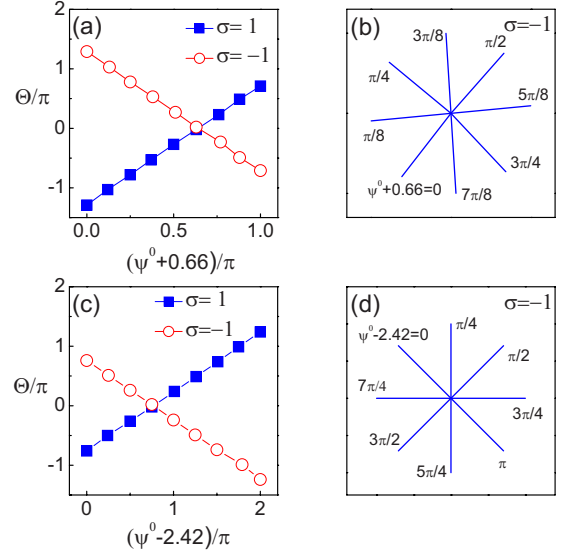


FIG. 6. (Color online) [(a) and (b)] Dependence of the drift of a single-armed spiral by a periodic advective field ($\omega_e = 2\omega_0$, $E_f = 0.01$) on the initial phase of the spiral. [(c) and (d)] Dependence of the drift of single-armed spirals by periodic modulation of excitability ($\omega_b = \omega_0$, $b_f = 0.003$) on the initial phase of the spiral.

separated in equal phase, we have $|\psi_2^0 - \psi_1^0| \simeq \pi$. Consequently, the drift directions of the two tips are almost the same since $|\Theta_2 - \Theta_1| = 2|\psi_2^0 - \psi_1^0| \simeq 2\pi$. This is why the two tips of a two-armed spiral drift in the same direction under the influence of a periodic advective field with $\omega_e = 2\omega_0$, see Fig. 2(a). From Eq. (10), one can see that only the tips of two-armed spirals drift in the same direction. The tips of other multiarmed (e.g., three- or four-armed) spirals will drift in different directions.

Following the same strategy, we can also derive the drift behavior of the spiral tips when the medium excitability is resonantly modulated by setting parameter $b = b_0 + b_f \cos(\omega_0 t + \varphi)$. According to Eq. (7), the radial motion of the $j$th tip satisfies

$$\ddot{r}_j + \omega_0^2 r_j = \omega_0^2 \left. \frac{\partial R_j}{\partial b} \right|_{b_0} b_f \cos(\omega_0 t + \varphi). \tag{12}$$

The solution can be written as $r_j(t) = 1/2(\partial R_j / \partial b)_{b_0} b_f \omega_0 t \sin(\omega_0 t + \varphi)$. It gives a linear drift of the rotation center of the $j$th tip, which can be written as [27,32]

$$z_j^0(t) = \frac{1}{2} \left. \frac{\partial R_j}{\partial b} \right|_{b_0} b_f \omega_0 t \exp[i\sigma(\pi/2 - \varphi + \psi_j^0)]. \tag{13}$$

Different from the case of periodic advective field, the drift direction depends on the initial phase of spiral tip by one time, $\Theta_j = \sigma(\pi/2 - \varphi + \psi_j^0)$, and thus we have

$$|\Delta \Theta_j| = |\Delta \psi_j^0|, \tag{14}$$

which explains the numerical results observed in Figs. 4(c) and 4(d). In Figs. 6(c) and 6(d), the relation between the drift direction and the initial phase of a single-armed spiral tip is given. One can see that the numerical results agree well with

the analytic results. For a rigidly rotating two-armed spiral with tips separated in equal phase, the difference of drift directions $|\Theta_2 - \Theta_1|$ equals to the difference of the initial phases of the two tips $|\psi_2^0 - \psi_1^0| \simeq \pi$. That is the reason why the two tips of a two-armed spiral drift in the opposite direction when the excitability is modulated periodically with $\omega_b = \omega_0$, see Fig. 4(a).

Note that the initial phase of spiral tip was not taken into account (was taken as zero) in Ref. [27] in deriving the drift of single-armed spiral under external actions. Here, we see that the initial phase plays an important role in explaining our numerical results, see Eqs. (10) and (13) for details. Under weak deformation approximation, we derived approximate formulae of drift velocities of dense spirals under external actions [28,30]. Thus, it is not suitable to study the drift of spirals in weakly excitable media by using these formulae. Nevertheless, the numerical results observed in this paper can also be explained qualitatively by using these approximate formulae. In Ref. [28], we gave the drift velocity of a spiral induced by a periodic advective field with $\omega_e = 2\omega_0$, from which we can get the drift directions of the two tips: $\tan \Theta_j = -\sigma \tan(\varphi + \alpha_j + \beta_j + \pi/2)$, $j = 1, 2$. Here $\alpha_j$ and $\beta_j$ are two phase shifts and $|\Delta\alpha_j| = |\Delta\beta_j| = |\Delta\psi_j^0|$. If the change of the initial phase is $|\Delta\psi_j^0|$, then we have $|\Delta\Theta_j| = |\Delta\alpha_j + \Delta\beta_j| = 2|\Delta\psi_j^0|$, which is consistent with Eq. (11). In Ref. [30], we derived the drift velocity of a spiral when the medium is resonantly modulated ($\omega_b = \omega_0$) and we can obtain

the drift directions of the two tips: $\tan \Theta_j = -\sigma \tan(\varphi + \alpha_j - \pi/2)$, $j = 1, 2$; thus we have $|\Delta\Theta_j| = |\Delta\alpha_j| = |\Delta\psi_j^0|$, which is consistent with Eq. (14).

## IV. CONCLUSIONS

We have investigated the resonant drift of two-armed spirals by periodic advective field and periodic modulation of excitability. When controlled by a periodic advective field with $\omega_e = 2\omega_0$, the two tips of the two-armed spiral drift in the same direction and the two-armed spiral remain stable. When the excitability is modulated periodically with $\omega_b = \omega_0$, the two tips drift in the opposite direction and two-armed spiral splits into two single-armed spirals if the strength of the modulation is strong. If the modulation is weak, the two-armed spiral will not split and the two tips meander around each other. All simulation results are consistent with the theoretical analysis based on a kinematic theory of rotating spirals in weakly excitable media. Our theoretical results is expected to be observed in experiments, such as the BZ reaction.

[1] J. M. Davidenko, A. V. Pertsov, R. Salomonsz, W. Baxter, and J. Jalife, Nature (London) **355**, 349 (1992).

[2] F. Siegert and C. Weijer, J. Cell Sci. **93**, 325 (1989).

[3] N. A. Gorelova and J. Bures, J. Neurobiol. **14**, 353 (1983).

[4] A. T. Winfree, Science **175**, 634 (1972).

[5] S. Jakubith, H. H. Rotermund, W. Engel, A. von Oertzen, and G. Ertl, Phys. Rev. Lett. **65**, 3013 (1990).

[6] For reviews, see Focus Issue: on Fibrillation in Normal Ventricular Myocardium, Chaos **8**(1) (1998); Focus Issue: on Mapping and Control Cardiac Arrhythmias, *ibid.* **12**(3) (2002); Focus Issue: on Cardiovascular Physics, *ibid.* **17**(1) (2007).

[7] R. A. Gray, A. M. Pertsov, and J. Jalife, Nature (London) **392**, 75 (1998).

[8] F. X. Witkowski, L. J. Leon, P. A. Penkoske, W. R. Giles, M. L. Spano, W. L. Ditto, and A. T. Winfree, Nature (London) **392**, 78 (1998).

[9] S. Alonso, F. Sagués, and A. S. Mikhailov, Science **299**, 1722 (2003).

[10] H. Zhang, Z. Cao, N. J. Wu, H. P. Ying, and G. Hu, Phys. Rev. Lett. **94**, 188301 (2005).

[11] K. I. Agladze and V. I. Krinsky, Nature (London) **296**, 424 (1982).

[12] O. Steinbock and S. C. Müller, Int. J. Bifurcation Chaos Appl. Sci. Eng. **3**, 437 (1993).

[13] S. Nettesheim, A. von Oertzen, H. H. Rotermund, and G. Ertl, J. Chem. Phys. **98**, 9977 (1993).

[14] B. Vasiev, F. Siegert, and C. Weijer, Phys. Rev. Lett. **78**, 2489 (1997).

[15] T. J. Wu, M. A. Bray, C. T. Ting, and S. F. Lin, J. Cardiovasc. Electrophysiol. **13**, 414 (2002).

[16] N. Bursac, F. Aguel, and L. Tung, Proc. Natl. Acad. Sci. U.S.A. **101**, 15530 (2004).

[17] E. A. Ermakova, A. M. Pertsov, and E. E. Shnol, Physica D **40**, 185 (1989).

[18] R. M. Zaritski, J. Ju, and I. Ashkenazi, Int. J. Bifurcation Chaos Appl. Sci. Eng. **15**, 4087 (2005).

[19] C. W. Zemlin, K. Mukund, V. N. Biktashev, and A. M. Pertsov, Phys. Rev. E **74**, 016207 (2006); C. Zemlin, K. Mukund, M. Wellner, R. Zaritsky, and A. Pertsov, Phys. Rev. Lett. **95**, 098302 (2005).

[20] For examples, see A. Schrader, M. Braune, and H. Engel, Phys. Rev. E **52**, 98 (1995); V. S. Zykov, O. Steinbock, and S. C. Müller, Chaos **4**, 509 (1994); R. M. Mantel and D. Barkley, Phys. Rev. E **54**, 4791 (1996); I. V. Biktasheva and V. N. Biktashev, *ibid.* **67**, 026221 (2003).

[21] For examples, see K. I. Agladze and P. De Kepper, J. Phys. Chem. **96**, 5239 (1992); V. Krinsky, E. Hamm, and V. Voignier, Phys. Rev. Lett. **76**, 3854 (1996); H. Henry, Phys. Rev. E **70**, 026204 (2004); J. X. Chen, H. Zhang, and Y. Q. Li, J. Chem. Phys. **124**, 014505 (2006).

[22] K. I. Agladze, V. A. Davydov, and A. S. Mikhailov, JETP Lett. **45**, 767 (1987).

[23] O. Steinbock, J. Schütze, and S. C. Müller, Phys. Rev. Lett. **68**, 248 (1992).

[24] A. P. Muñuzuri, M. Gómez-Gesteira, V. Pérez-Muñuzuri, V. I. Krinsky, and V. Pérez-Villar, Phys. Rev. E **50**, 4258 (1994).

[25] D. Barkley, M. Kness, and L. S. Tuckerman, Phys. Rev. A **42**, 2489 (1990).

[26] L. Y. Deng, H. Zhang, and Y. Q. Li, Phys. Rev. E **79**, 036107 (2009).

[27] V. Hakim and A. Karma, Phys. Rev. E **60**, 5073 (1999).

[28] H. Zhang, B. Hu, G. Hu, and J. Xiao, J. Chem. Phys. **119**, 4468 (2003).

[29] See A. S. Mikhailov, V. A. Davidov, and V. A. Zykov, Physica

[30] H. Zhang, N. J. Wu, H. P. Ying, G. Hu, and B. Hu, J. Chem. Phys. **121**, 7276 (2004).

[31] M. Bär, N. Gottschalk, M. Eiswirth, and G. Ertl, J. Chem. Phys. **100**, 1202 (1994).

[32] V. Hakim, private communication. Equation (126) of [27] should be $z_0 = \frac{3}{4} R_0 \frac{A}{B_c - B} \omega_1 t[i \exp(-i\phi)]$.

D **70**, 1 (1994), and references therein.